

## Selective Nontemplated Adsorption of Organic Molecules on Nanofacets and the Role of Bonding Patterns

S. X. Du,<sup>1,2</sup> H. J. Gao,<sup>1,\*</sup> C. Seidel,<sup>3</sup> L. Tsetseris,<sup>4</sup> W. Ji,<sup>1</sup> H. Kopf,<sup>3</sup> L. F. Chi,<sup>3</sup> H. Fuchs,<sup>3</sup>  
S. J. Pennycook,<sup>2,4</sup> and S. T. Pantelides<sup>4,2,†</sup>

<sup>1</sup>National Laboratory of Condensed Matter Physics, Institute of Physics, Chinese Academy of Sciences,  
P.O. Box 603, Beijing 100080, China

<sup>2</sup>Materials Science and Technology Division, Oak Ridge National Laboratory, Oak Ridge, Tennessee 37831, USA

<sup>3</sup>Physics Institute, University of Münster, D-48149 Münster, Germany

<sup>4</sup>Department of Physics and Astronomy, Vanderbilt University, Nashville, Tennessee 37235, USA

(Received 11 August 2006; published 13 October 2006)

A key element of functionalizing nanocrystals with organic molecules is the nontemplated selective adsorption of different molecules on different facets. Here we report scanning-tunneling-microscopy images of perylene-3,4,9,10-tetracarboxylic-dianhydride and 2,5-dimethyl-*N,N'*-dicyanoquinonediimine on silver, demonstrating selective adsorption on different facets. We also report first-principles calculations that account for the data and show that bonding, which controls selectivity, occurs via the end atoms, while the molecule's midregion arches away from the substrate. The results are also consistent with data that have been interpreted in terms of bonding via the midregion.

DOI: [10.1103/PhysRevLett.97.156105](https://doi.org/10.1103/PhysRevLett.97.156105)

PACS numbers: 68.43.Fg

Many nanocrystal applications require adsorption of organic molecules [1–6]. Controlled selective adsorption of different molecules on different facets would enhance significantly the design of functionality [7–9]. As a result, the adsorption of organic molecules on crystal surfaces has been investigated extensively, leading to several conclusions about bonding mechanisms [10–13]. A prototype system is perylene-3,4,9,10-tetracarboxylic-dianhydride (PTCDA), which forms an ordered monolayer on Ag(111) surfaces [13,14]. PTCDA consists of seven benzene rings with H terminators at the long sides and O terminators at the short sides [Fig. 2(a)]. Experimental data and theoretical calculations have led to the conclusion that PTCDA and similar molecules bond to the substrate primarily via the midregion  $\pi$ -electron system [15–20].

In this Letter, we report the results of experiments that were designed to probe the selective adsorption of PTCDA and 2,5-dimethyl-*N,N'*-dicyanoquinonediimine (DMe-DCNQI) on (111) and (221) facets of a single Ag(775) substrate. We show that, upon annealing, PTCDA adsorbs preferentially on the (111) facet, while DMe-DCNQI adsorbs preferentially on the (221) facet. By varying the relative amounts, the sequence of deposition, and annealing, it is possible to get each molecule to form an ordered structure exclusively on its preferred facet. We also report first-principles density-functional calculations of PTCDA, DMe-DCNQI, and other similar molecules on facets with varying terrace widths and step heights. We find that the binding energy of PTCDA is larger on the flat (111) facet, whereas the binding energy of DMe-DCNQI is larger on the stepped (221) facet, in agreement with observations. The results of the calculations elucidate the bonding mechanisms and lead to simple rules that govern the se-

lective adsorption. In all cases, bonding occurs through only the end atoms, while the midregion benzene rings arch away from the substrate (if the end O are removed, the molecule flattens and stabilizes at a larger molecule-substrate distance). By the same token, the availability of a step of appropriate height may enhance the bonding by lifting one end and flattening the molecule, but only if the terrace is wide enough to accommodate the length of the molecule. These results contrast with the conclusions reached in prior work that aromatic molecules bond to the substrate primarily through their midregion  $\pi$ -electron system [15–20]. We reexamine the evidence that led to those conclusions and show that it can be reinterpreted in terms of the new results.

Experiments were carried out on a Ag(775) substrate, which displays two distinct types of facets, flat (111) facets and stepped (221) facets. The substrate was oriented by a Laue back-reflection pattern and polished. It was subsequently cleaned by cycles of Ar<sup>+</sup> sputtering for 20 min at 500 eV and annealed up to 700 K in the UHV chamber. Crystallographic order and cleanliness of the substrate were checked by low energy electron diffraction (LEED) and x-ray photoelectron spectroscopy. The molecules were deposited in an ultrahigh-vacuum chamber outfitted with a molecular beam epitaxy and low energy electron diffraction analytical capabilities. Two different sequences were executed. First, PTCDA was deposited at room temperature. Molecules were adsorbed on both facets, but LEED analysis revealed an ordered structure on only the (221) facet. Subsequent deposition of DMe-DCNQI led to a disappearance of the ordered structure. Finally, annealing at 330 K resulted in only PTCDA on the (111) facets, with a mixture of both molecules on the (221) facets. Scanning-

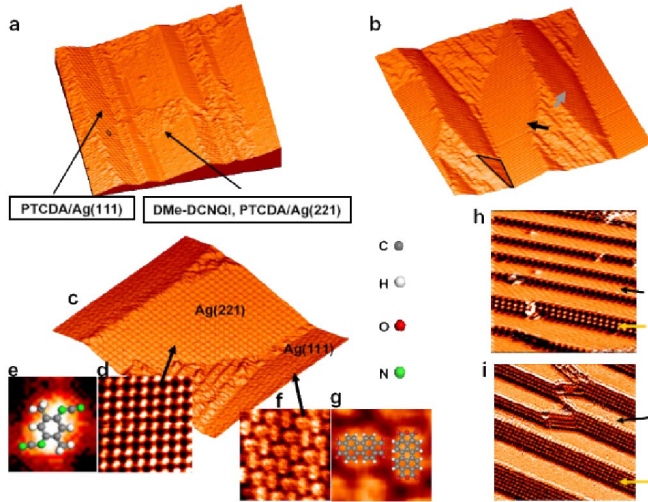


FIG. 1 (color online). STM images of PTCDA and DMe-DCNQI on a Ag(775) substrate. (a)  $30 \text{ nm} \times 30 \text{ nm}$  image of DMe-DCNQI and PTCDA, evaporating PTCDA first. The molecules are coadsorbed on (221) facets, while (111) facets are covered with PTCDA molecules (oval). (b)  $50 \text{ nm} \times 50 \text{ nm}$  image of DMe-DCNQI and PTCDA, evaporating DMe-DCNQI first. DMe-DCNQI adsorbed on the (221) facet (dark arrow), while PTCDA adsorbed on the (111) facet (gray arrow). Uncovered (111) areas are visible (triangular frame). (c)  $30 \text{ nm} \times 30 \text{ nm}$  image of DMe-DCNQI/Ag(221) and PTCDA/Ag(111). (d)  $6 \text{ nm} \times 6 \text{ nm}$  image of DMe-DCNQI on Ag(221). (e) Schematic structure of DMe-DCNQI/Ag(221) superimposed on the STM image (orientation determined from the STM image). (f)  $6 \text{ nm} \times 6 \text{ nm}$  image of PTCDA on Ag(111). (g) Schematic structure of PTCDA/Ag(111) superimposed on the STM image (orientation determined from the STM image). (h),(i) Images ( $20 \text{ nm} \times 20 \text{ nm}$  and  $30 \text{ nm} \times 30 \text{ nm}$ , respectively) of only DMe-DCNQI evaporated, shown adsorbed only on Ag(221) facets [light (yellow) arrows]; Ag(111) facets are bare (black arrows). The tunneling current is  $0.1 \text{ nA}$  and the sample bias is  $0.8 \text{ V}$  for all the STM images.

tunneling-microscopy (STM) images are shown in Fig. 1(a). By controlling the total quantity of each deposited molecule, it was possible to get PTCDA exclusively on (111) facets and DMe-DCNQI exclusively on (221) facets. In the second sequence, the molecules were deposited in the reverse order. First, DMe-DCNQI was deposited at room temperature, but no ordered structures were found by LEED. PTCDA was deposited next, and the system was annealed at  $340 \text{ K}$ . The final result was ordered monolayers of PTCDA exclusively on (111) facets and DMe-DCNQI exclusively on (221) facets [Figs. 1(b)–1(g)]. LEED analysis at different energies confirmed the ordered structures on the two facets. In a final experiment, only DMe-DCNQI was deposited, and the sample was annealed at  $318 \text{ K}$ . The molecule adsorbed exclusively on (221) terraces [Figs. 1(h) and 1(i)].

Theoretical calculations were based on density-functional theory, the Perdew-Wang exchange-correlation functional with generalized-gradient corrections [21], ul-

trasoft pseudopotentials [22], and plane waves, as implemented in the VASP code [23,24]. Supercells containing six Ag layers and  $1.2 \text{ nm}$  of vacuum were used. Bonding configurations were investigated for high coverage, namely, two molecules per  $4 \times 8$  surface Ag atoms, and a lower coverage, namely, one molecule per  $4 \times 7$  surface Ag atoms. An energy cutoff of  $400 \text{ eV}$  was used after convergence tests showed it to be adequate. The use of a higher cutoff of  $500 \text{ eV}$  for selected cases confirmed convergence for bonding configurations, in particular, the presence of arching. Each molecule was placed on the surface, and all atoms except for the bottom two Ag layers were relaxed until the net force on every atom was smaller than  $0.02 \text{ eV}/\text{\AA}$ .

Results for PTCDA and DMe-DCNQI are shown in Figs. 2(a) and 2(b). After relaxation, ordered PTCDA molecules are at right angles as in the image of Fig. 1(g) (ordered layers at other angles are at higher energies at  $T = 0 \text{ K}$ ). In addition, PTCDA binds more strongly on the (111) facet over the (221) facet ( $0.54$  versus  $0.22 \text{ eV}$ ); DMe-DCNQI forms even stronger bonds on either of the facets, with a small preference for the stepped (221) facet ( $1.46$  versus  $1.36 \text{ eV}$ ). The calculated binding energies are consistent with and account for the STM data. The small binding energy of PTCDA plays a role in the molecules' ability to migrate and form ordered structures at room temperature, while the same is not true for DMe-DCNQI, as observed. Indeed, when DMe-DCNQI is deposited first, it does not form ordered structures. When it is deposited second, it disorders the previously deposited PTCDA layers. Annealing at elevated temperatures, however, allows both molecules to migrate and sample the two types of facets. It is clear from the data that, when PTCDA is available in sufficient quantities, it dominates the (111) facets because of the larger energy gain. The small difference between the DMe-DCNQI binding energies on (111) and (221) facets, only  $0.1 \text{ eV}$ , is comparable to the numerical uncertainty of the calculations, but it appears to be real. At the experimental temperatures, close to room temperature, the preference for the (221) facet is  $e^4$  or close to  $1:60$ , which is consistent with the data.

In order to probe the bonding mechanisms that control selectivity, we obtained equilibrium configurations for DMe-DCNQI on varying terrace widths and step heights, shown in Fig. 2(b). PTCDA is too large for such calculations. Instead, we studied NTCDA, which is the same as PTCDA, but with only four instead of seven benzene rings. The results of Fig. 2 and similar results for NTCDA, show clearly that bonding occurs via the end atoms, with the benzene-ring cores always arching away from the substrate. This tendency is exploited at stepped edges, where bonding is enhanced. It is found that bonding is maximal for a terrace that is four atoms wide and a single-atom step. Making the step higher than a monolayer or the terrace wider than four atoms does not help (in addition, molecules do not like to straddle the step and have the step poking at

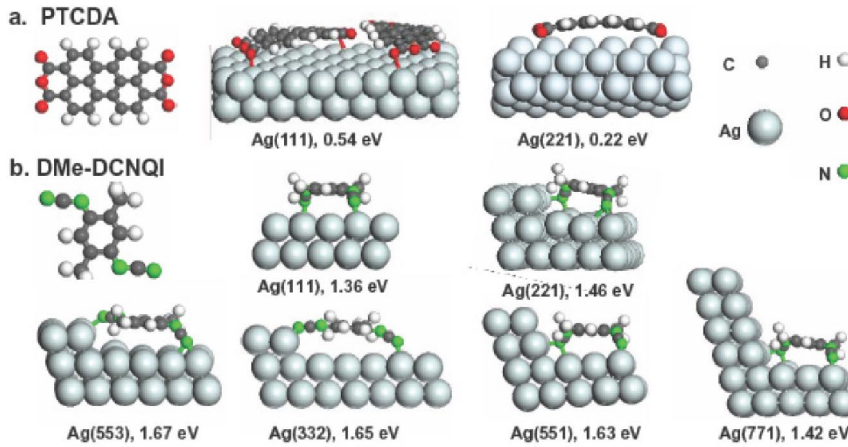


FIG. 2 (color online). Optimized configurations of (a) PTCDA and (b) DMe-DCNQI on the Ag(111) surface and on various stepped surfaces. Binding energies are indicated.

their midregion). Indeed, note that a DMe-DCNQI molecule fits comfortably on the (221) terrace width and gets extra bonding on the step edge, explaining the slight preference for the stepped facet. In contrast, the longer PTCDA molecule does not fit on the terrace width and turns sideways, with its H terminators alongside the step edge lifting that side of the molecule up somewhat, but the O terminators cannot reach the step for extra bonding. Instead, bonding is weakened by the presence of the step. It is clear that the binding energy would be enhanced if the terrace were wider and the molecule could fit longwise with the O terminators of one end bonding to the step edge, as in the case of DMe-DCNQI in Fig. 2(b). Indeed, unlike PTCDA, which turns sidewise on the narrow (221) terraces, NTCDA bonds longwise, taking advantage of the step. The trend is confirmed by results for even wider terraces on (332) facets, where the three end O atoms bond strongly to the step.

Our conclusion that bonding is through the end O or N atoms, while the midregion is repelled by the substrate contrasts with conclusions reached in a series of papers [15–20] that bonding is primarily via the benzene-ring  $\pi$  electrons. We will now show that all the data used in Refs. [15–20] are consistent with our theoretical results. In Ref. [20], it was found that the near-edge peak in the carbon  $K$  x-ray absorption spectrum of a monolayer of PTCDA molecules splits into two peaks in a thick film. This result was interpreted in terms of midregion C atoms bonding to the substrate [18–20]. We calculated C  $K$  x-ray absorption spectra in the “ $Z + 1$  approximation” [25–27] of an adsorbed PTCDA monolayer and a molecular crystal of PTCDA and found excellent agreement with the experimental spectra (Fig. 3), demonstrating that the data do not constitute evidence for midregion bonding.

In Ref. [17], it was shown that four Raman modes, which in free molecules correspond to breathing of the midregion C rings, are significantly enhanced in PTCDA adsorbed on silver. The authors suggested that the enhancement implies midregion bonding and, hence, charge transfer to the molecule, with the electromagnetic field driving the resulting dipole and the midregion Raman modes. Our calcula-

tions have shown that bonding occurs through the end atoms. We also find that charge transfer to the adsorbed molecule is negligible (Fig. 4). Nevertheless, the Ag-O-C bonds do have a nonzero dipole (simply because the positive and negative charges do not have identical distributions), whereby the midregion Raman modes can be driven by charge-pumping action through the Ag-O-C bonds. Thus, using the same qualitative reasoning employed in Ref. [17], we conclude that our results are equally consistent with the Raman data.

In a recent Letter [19], new experimental data and theoretical calculations on adsorbed PTCDA molecules were reported. The theoretical results were subsequently found to be artifacts of certain approximations [28,29]. In revised results [29], the authors find negligible charge transfer in the midregion, eliminating the original argument [19] in favor of midregion bonding. In Ref. [19], “coherent distances” of O and C atoms from the surface were extracted from the data. We calculated coherent distances and found that the O values are in excellent agreement with the values extracted from experimental data in Ref. [19]. The theoretical values for C reflect arching and range from 3.2 to 3.6 Å, in contrast to the single value of 2.86 Å extracted from the data in Ref. [19]. We note, however, that in Fig. 2 of Ref. [19] the C spectrum has a relatively flat top, which is indicative of a range of C

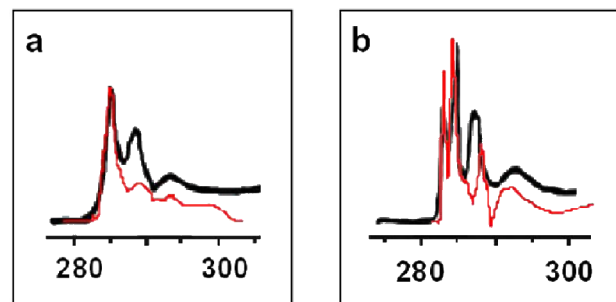


FIG. 3 (color online). Experimental C  $K$ -edge x-ray absorption spectra (black lines) of (a) monolayer and (b) thick-film PTCDA on Ag(111). Theoretical spectra [light (red) lines] of (a) monolayer and (b) molecular crystal.

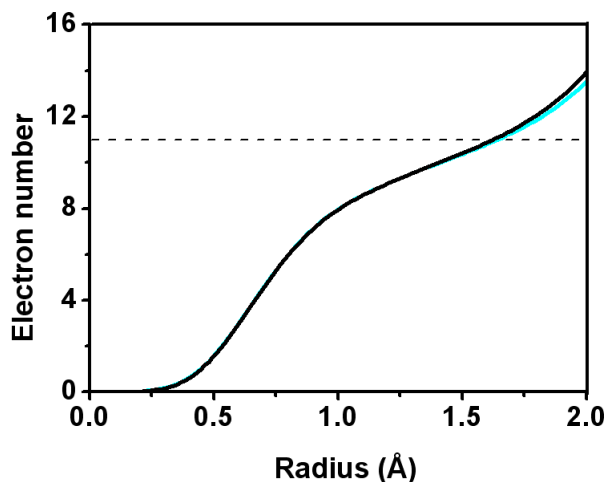


FIG. 4 (color online). Spherically integrated valence electron density around different Ag atoms as a function of the integration radius. Ag atoms in the bulk (black line) and at the surface below the PTCDA midregion [light (cyan) line] are shown. The dotted line indicates the number of valence electrons in a neutral Ag atom.

distances, consistent with the arching found in our calculations. It is clear that the data need to be reanalyzed by assuming arching, more specifically to check if the predicted C distances, which at this point appear somewhat large, are in fact consistent with the data. We close by noting that our theoretical results differ in detail from those of Refs. [28,29]. The methods of those Letters are based on specific choices of localized basis sets. The present results are fully converged with respect to the number of basis functions. We tested configurations for flat molecules on fixed substrates, similar to those described in Refs. [28,29], and found that they are generally metastable,  $\sim 0.2$  eV higher in energy than the arched configuration. Relaxation of both the molecule and the substrate enhances arching. Recent results [30] on NTCDA adsorption on Ag(110) surfaces are consistent with our conclusions.

In conclusion, we have demonstrated that organic molecules bond preferentially to different facets of an Ag substrate and that the controlling factors are the relative lengths of the molecules, terrace widths, and the heights of step edges. Molecules with O or N at the ends bond to the substrate via these end atoms, while midregion benzene rings do not contribute to bonding. A step edge at one end of the molecule strengthens bonding. We expect that these results can form a framework for the design of nontemplated selective functionalization of nanocrystals.

This work was supported in part by the National Science Foundation of China, Chinese National 863 and 973 projects, by the Chinese Academy of Sciences, by the U.S. Department of Energy under Contract No. DE-AC05-00OR22725 at ORNL, managed by UT/Battelle, by the McMinn Endowment at Vanderbilt University, and

by the Ministry of Science and Research (MWF), Northrhine Westfalia, Germany.

\*Electronic address: hjgao@aphy.iphy.ac.cn

†Electronic address: pantelides@vanderbilt.edu

- [1] R. P. Andres *et al.*, *Science* **273**, 1690 (1996).
- [2] Y. C. Cao, R. Jin, and C. A. Mirkin, *Science* **297**, 1536 (2002).
- [3] S. M. Nie and S. R. Emery, *Science* **275**, 1102 (1997).
- [4] W. H. Guo, J. J. Li, Y. A. Wang, and X. G. Peng, *J. Am. Chem. Soc.* **125**, 3901 (2003).
- [5] M. C. Schlamp, X. G. Peng, and A. P. Alivisatos, *J. Appl. Phys.* **82**, 5837 (1997).
- [6] G. Medeiros-Ribeiro *et al.*, *Phys. Rev. B* **59**, 1633 (1999).
- [7] A. K. Salem, P. C. Searson, and K. W. Leong, *Nat. Mater.* **2**, 668 (2003).
- [8] W. A. Germishuizen *et al.*, *Nanotechnology* **14**, 896 (2003).
- [9] L. Gross *et al.*, *Chem. Phys. Lett.* **371**, 750 (2003).
- [10] G. Horowitz, *Adv. Mater.* **10**, 365 (1998).
- [11] S. Forrest, P. Burrows, and M. Thompson, *IEEE Spectrum* **37**, 29 (2000).
- [12] S. R. Forrest, *Chem. Rev.* **97**, 1793 (1997).
- [13] E. Umbach *et al.*, *Surf. Sci.* **402**, 20 (1998).
- [14] B. Krause *et al.*, *Appl. Surf. Sci.* **175**, 332 (2001).
- [15] F. S. Tautz, M. Eremtchenko, J. A. Schaefer, M. Sokolowski, V. Shklover, and E. Umbach, *Phys. Rev. B* **65**, 125405 (2002).
- [16] F. S. Tautz, M. Eremtchenko, J. A. Schaefer, M. Sokolowski, V. Shklover, K. Glockler, and E. Umbach, *Surf. Sci.* **502**, 176 (2002).
- [17] M. Eremtchenko, D. Bauer, J. A. Schaefer, and F. S. Tautz, *New J. Phys.* **6**, 4 (2004).
- [18] M. Eremtchenko, J. A. Schaefer, and F. S. Tautz, *Nature (London)* **425**, 602 (2003).
- [19] A. Hauschild, K. Karki, B. C. C. Cowie, M. Rohlfing, F. S. Tautz, and M. Sokolowski, *Phys. Rev. Lett.* **94**, 036106 (2005).
- [20] J. Taborski *et al.*, *J. Electron Spectrosc. Relat. Phenom.* **75**, 129 (1995).
- [21] J. P. Perdew *et al.*, *Phys. Rev. B* **46**, 6671 (1992).
- [22] D. Vanderbilt, *Phys. Rev. B* **41**, 7892 (1990).
- [23] G. Kresse and J. Furthmuller, *Phys. Rev. B* **54**, 11 169 (1996).
- [24] G. Kresse and J. Hafner, *Phys. Rev. B* **47**, 558 (1993).
- [25] R. Buczko, G. Duscher, S. J. Pennycook, and S. T. Pantelides, *Phys. Rev. Lett.* **85**, 2168 (2000).
- [26] G. Duscher, R. Buczko, S. J. Pennycook, and S. T. Pantelides, *Ultramicroscopy* **86**, 355 (2001).
- [27] S. T. Pantelides *et al.*, in *Fundamental Aspects of Silicon Oxidation*, edited by Y. J. Chabal (Springer, New York, 2000), p. 193.
- [28] R. Rurali, N. Lorente, and P. Ordejón, *Phys. Rev. Lett.* **95**, 209601 (2005).
- [29] A. Hauschild, K. Karki, B. C. C. Cowie, M. Rohlfing, F. S. Tautz, and M. Sokolowski, *Phys. Rev. Lett.* **95**, 209602 (2005).
- [30] A. Alkaskas, A. Baratoff, and C. Bruder, *Phys. Rev. B* **73**, 165408 (2006).